JOURNAL OF MATERIALS SCIENCE **34** (1999) 4457–4468

Weibull master curves and fracture toughness testing

Part IV *Dynamic fracture toughness of ferritic-martensitic steels in the DBTT-range*

M. LAMBRIGGER
Centre de recherches en physique des plasmas, Technologie de la Fusion, EPFL, Im Struppen 12, CH 8048 Zürich, Switzerland

Ferritic-martensitic steels are considered to be promising candidates for structural materials in fusion technology. However, they are sensitive to irradiation embrittlement, being characterized by a shift of the ductile-to-brittle transition temperature (DBTT) to higher values. It has already been shown in an earlier publication, that dynamic Weibull master curves are useful in estimating the capacity of materials to undergo stable (micro)cracking prior to brittle failure, if Charpy impact tests are performed in the DBTT-range. Thus, experimental dynamic Weibull master curves of three ferritic-martensitic steels, having been obtained by performing series of instrumented Charpy impact tests at a defined temperature in the DBTT-range, have been evaluated for subsize and, in the case of the reference ferritic-martensitic steel of the European Fusion Technology Program MANET II, for normal-size specimens. It has been observed, that the capacities of stable (micro)cracking of MANET II are nearly optimal and clearly superior to those of the other two considered steels. On the other side, the capacity of stable (micro)cracking prior to failure has been found to be highly specimen-size-dependent, nevertheless it is thought to be an important factor in predicting DBTT-shifts due to irradiation embrittlement.

Nomenclature

c	crack length
σ	applied failure stress or normal stress built up in the process zone
$P(\sigma)$	quasi-static, three-parameter, cumulative Weibull failure probability distribution function
m	quasi-static Weibull modulus
z	distinct value of the cumulative failure probability distribution function
τ	toughening exponent
P	pendulum force acting on the Charpy specimen
P'	reaction line-force built up at the notch-tip of the Charpy specimens during testing
m'	dynamic Weibull modulus
$P_{\max}$	maximum impact line-force built up during Charpy impact testing
$P(P_{\max})$	dynamic, two-parameter, cumulative Weibull failure probability distribution function
$P'_{\max}$	maximum reaction line-force at the notch-tip arising during Charpy impact testing
$P_{\max 0}$	normalizing factor in dimensions of load
$P_{\max \tau}$	threshold load-value, below which the cumulative probability of failure is 100%
$P_{\max z}$	maximum impact line-force corresponding to the cumulative failure probability z
$P_{\max in}$	maximum impact line-force at the inflexion point of the

0022–2461

	two-parameter, cumulative Weibull failure probability distribution function $P(P_{max})$
$\bar{P}_{max}$	mean-value of the maximum impact line force
$I(x', m')$, $K(y', m')$ and $M[e'(z), m']$	three different types of dynamic, theoretical Weibull master curves
$I\exp(x', m')$, $K\exp(y', m')$ and $M\exp[e'(z), m']$	three different types of dynamic, experimental Weibull master curves
x', y' and $e'(z)$	different types of scaled maximum impact line-forces
x'_{cr}, y'_{cr}, $e'_{cr}(z)$	values of the cross-over points formed by the corresponding experimental and theoretical master curves
$H'[e'(z)]$	step function, being equal to one for $e'(z) < e'_{cr}(z)$ and equal to zero for $e'(z) \geq e'_{cr}(z)$
$FiM1'[e'(z)]$, $FiM2'[e'(z)]$, $F\exp 1M'[e'(z)]$, $F\exp 2M'[e'(z)]$, $FiM1'[e'(z_{in})]$, $FiM2'[e'(z_{in})]$, $F\exp 1M'[e'(z_{in})]$, $F\exp 2M'[e'(z_{in})]$, $d\chi_M$, $d\chi_I$ and $d\chi_k$	deviation parameters derived from the step function $H'[e'(z)]$ and from the dynamic Weibull master curves

1. Introduction

9–12 wt % Cr ferritic-martensitic steels with fine carbide structures are considered as potential candidates for the blanket and first wall structures of a fusion reactor, mainly because of their high strength, low thermal dilatation and high resistance to void swelling. Extensive studies have already taken place in Japan, US and Europe [1]. Unfortunately, ferritic-martensitic steels are sensitive to embrittlement, if they are irradiated under a fusion neutron spectra. This irradiation embrittlement is characterized by a shift of the ductile-to-brittle transition temperature (DBTT) to higher values [2], usually being measured with the help of instrumented Charpy impact tests [3]. These tests are performed for definite materials at varying testing-temperatures, and provide the Charpy energies (absorbed impact energies) of the specimens as a function of the testing-temperatures. The Charpy energy is obtained by integration of the measured pendulum force P vs. time diagrams [3]. Charpy energy vs. temperature diagrams are generally used in order to characterize the ductile-to-brittle transition of ferritic-martensitic steels.

The reference ferritic-martensitic steel of the European Fusion Technology Program, the 10CrMoNbV MANET II, has been modified by replacing the elements Ni, Nb and Mo, which result in long term radioactivity, when irradiated under a fusion neutron spectra, at least partially by others being characterized by shorter activation periods. Thus, low activation steels, known as OPTIMAX steels, have been produced. Moreover, it has already been shown in part 3 of this series of papers [4], that dynamic Weibull master curves are useful in estimating the capacity of materials to undergo stable (micro)cracking prior to brittle failure, if Charpy impact tests are performed in the DBTT-range. These dynamic Weibull master curves can be obtained, if series of instrumented Charpy impact tests with a defined material at a fixed temperature in the DBTT-range are performed, and if the scatter of the pendulum force is studied according to the dynamic Weibull model presented in part 3 of this series of papers [4]. In this paper, experimental dynamic Weibull master curves of MANET II and two OPTIMAX steels have been evaluated for subsize and, in the case of MANET II, for normal-size specimens. The capacity of stable (micro)cracking prior to failure, being evaluated from these dynamic Weibull master curves, is considered to be an important factor in predicting DBTT-shifts of ferritic-martensitic steels due to irradiation embrittlement.

In part 3 [4], it has been shown, that it is possible to express the cumulative Weibull failure probability distribution $P(\sigma)$ also in terms of the maximum impact line-force P_{max}, if the threshold load-value $P_{max\,\tau}$ is equal to zero [4].

$$P(P_{max}) = 1 - \exp\left[-\left(\frac{P_{max}}{P_{max\,0}}\right)^{m'}\right] \tag{1}$$

whereby m' denotes a modified, dynamic Weibull modulus defined by

$$m' = m\frac{2\tau - 1}{2\tau + 1} \tag{2}$$

$P_{max\,0}$ represents a normalizing factor which has dimensions of load, m denotes the quasi-static Weibull modulus m and τ the toughening exponent, which characterizes the rate of toughening increase with increasing crack length c [4–7].

In part 3 of this series of papers [4], it has been displayed that the three types of dynamic Weibull master curves $M[e'(z), m']$, $I(x', m')$ and $K(y', m')$ are easily derived from the two-parameter cumulative failure probability distribution function $P(P_{max})$ by defining the scaled, dynamic variables $e'(z)$, x' and y' as follows;

$$e'(z) = \frac{P_{max}}{P_{max\,z}}; \quad x' = e'(z_{in}) = \frac{P_{max}}{P_{max\,in}}; \quad y' = e'(\bar{z}) = \frac{P_{max}}{\bar{P}_{max}} \tag{3}$$

whereby z_{in} and $\bar{z}$ are directly defined by Equation 3, $P_{max\,z}$ denotes the maximum impact line-force corresponding to the cumulative failure probability z, $P_{max\,in}$ the maximum impact line-force at the inflexion point of $P(P_{max})$ and $\bar{P}_{max}$ the mean-value of the maximum impact line-force.

$$\bar{P}_{\max} = \int_0^1 P_{\max}\, dP = P_{\max 0}\Gamma\left(1 + \frac{1}{m'}\right) \quad (4)$$

$$P_{\max \text{in}} = P_{\max 0}\left[\frac{m'-1}{m'}\right]^{1/m'} \quad (5)$$

$M[e'(z), m']$ and $P_{\max z}$ exist for every real dynamic Weibull modulus m', however, $I(x', m')$ and $P_{\max \text{in}}$ are only real and positive for $m' < 0$ and $m' > 1$. The complete Gamma-function $\Gamma(1 + \frac{1}{m'})$ has already been discussed in part 1 of this series of papers [6], whereby m has to be replaced by m' in Equation 6 of part 1, if dynamic conditions are considered. $K(y', m')$ always exists for $m' < -1$ and $m' > 0$, since the complete Gamma-function is always real and positive in these cases. The dynamic Weibull master curves are mathematically given by

$$\begin{aligned} P(P_{\max}) &= M[e'(z), m'] \\ &= 1 - \exp\{\ln(1 - z)[e'(z)]^{m'}\} \\ &= 1 - (1 - z)^{[e'(z)]^{m'}} \end{aligned} \quad (6)$$

$$P(P_{\max}) = I(x', m') = 1 - \exp\left[\frac{(1-m')}{m'} x'^{m'}\right] \quad (7)$$

$$\begin{aligned} P(P_{\max}) &= K(y', m') \\ &= 1 - \exp\left\{-\left[\Gamma\left(1 + \frac{1}{m'}\right)\right]^{m'} y'^{m'}\right\} \end{aligned} \quad (8)$$

Besides, Equations 1–15, 26–34 and 38–43 of part 1 [6] as well as Equations 2–16 of part 2 [5], being defined for quasi-static constants, quasi-static variables and quasi-static (theoretical and experimental) Weibull master curves, are also true for dynamic (theoretical and experimental) Weibull master curves, if the quasi-static variables and quasi-static constants are replaced by the corresponding dynamic ones as described in part 3 of this series of papers [4].

Under dynamic loading conditions experimental failure data of Charpy impact tests ($P_{\max_i}$, $P(P_{\max_i})$) are evaluated with the help of a step function $H'[e'(z)]$, which equals one for $e'(z) < e'_{\text{cr}}(z)$ and zero for $e'(z) \geq e'_{\text{cr}}(z)$; $e'_{\text{cr}}(z)$ is representing the $e'(z)$-value corresponding to the cross-over point of the experimental dynamic Weibull master curve $M \exp[e'(z), m']$ and the corresponding theoretical dynamic Weibull master curve $M[e'(z), m']$. The two areas formed between the step function $H'[e'(z)]$ and $M[e'(z), m']$ are denoted by $FiM1'[e'(z)]$ and $FiM2'[e'(z)]$. $F \exp 1M'[e'(z)]$ and $F \exp 2M'[e'(z)]$ represent the two areas formed between $M \exp[e'(z), m']$ and $M[e'(z), m']$. With the help of $FiM1'[e'(z)]$, $FiM2'[e'(z)]$, $F \exp 1M'[e'(z)]$ and $F \exp 2M'[e'(z)]$ material-specific double-quotients $d\chi_M$, characterizing the dynamic toughening potential of the investigated materials, can be defined [4]:

$$d\chi_M = \frac{FiM1'[e'(z)]}{FiM2'[e'(z)]} : \frac{F \exp 1M'[e'(z)]}{F \exp 2M'[e'(z)]} \quad (9)$$

The dynamic, material-specific double-quotients $d\chi_I$ and $d\chi_k$ for the special, dynamic Weibull master curves $I(x', m')$ and $K(y', m')$ are obtained by replacing z by z_{in} or $\bar{z}$ in Equation 9.

2. Experimental

Subsize $3 \times 4 \times 27$ mm impact bend specimens of type DIN 50115 KLST with a V-notch of 1 mm parallel to the 3 mm edge forming an angle of 60°, have been tested using a fully instrumented Messtek-Amsler PHR1010 Charpy machine equipped with an automatic loading, heating and cooling system SFL-R1050. The radius at the notch-tip of these subsize specimens has been 0.1 mm. A tup speed of 3.59 m/s has been chosen for all the Charpy impact tests, having been performed with subsize specimens of MANET II, OPTIMAX A renorm. and OPTIMAX B. For the testing of the $10 \times 10 \times 55$ mm normal-size ISO-V specimens with a V-notch of 2 mm forming an angle of 45°, an instrumented standard H. Schnadt machine, built under licence by Mohr and Federhaff, has been used. The pendulum allowed testing in the range of 2.23 to 5.0 m/s by choosing convenient pendulum drop heights. A tup velocity of 3 m/s has been chosen for the Charpy impact testing of MANET II. The radius at the notch-tip of these MANET II normal-size specimens has been 0.25 mm.

Charpy impact tests at varying testing-temperatures have been performed with all the investigated ferritic-martensitic steels using subsize specimens. The measured Charpy energy (absorbed impact energy) vs. temperature diagrams are displayed in Fig. 1. Moreover, the scatter of the maximum pendulum force for a definite material at a fixed testing-temperature in the DBTT-range has been studied by performing series of instrumented Charpy impact tests. The dynamic Weibull master curves, which have been evaluated from these series of tests by registering the maximum impact line-force $P_{\max}$, are depicted in Figs 2 and 3 for subsize and normal-size specimens. Besides, the testing-temperatures and the tup speeds have been chosen in such a way that rupture always occured in a period of time, which made it possible to apply the dynamic Weibull model (i.e. the dynamic quasi-equilibrium approach described in part 3 [4]) to the evaluation of the Charpy impact testing data.

Alloy preparations and heat treatments of the reference ferritic-martensitic steel MANET II, the renormalized low activation ferritic-martensitic steel OPTIMAX A renorm. and the low activation ferritic-martensitic steel OPTIMAX B have already been described elsewhere [8, 9]. The chemical compositions are given in Table I.

3. Dynamic deviation parameters

The step function $H'[e'(z)]$ was introduced, because it represents formally an ideal material undergoing 0% unstable crack extension prior to rupture. Furthermore, ideal materials fail at $e'_{\text{cr}}(z)$ in a deterministic manner without undergoing any brittle cleavage fracture,

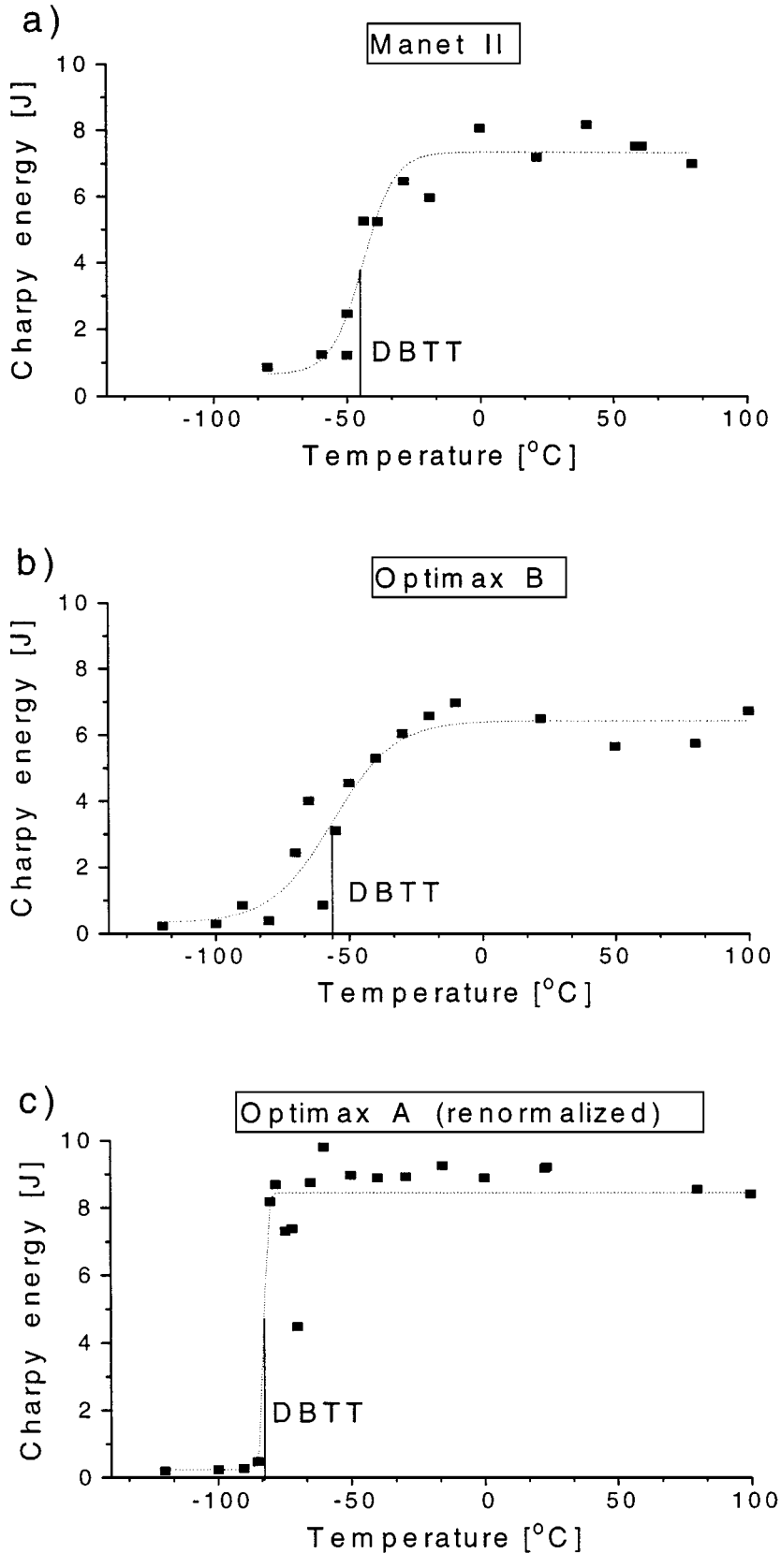

Figure 1 (a) Absorbed Charpy impact energy vs. testing-temperature diagram for subsize specimens of the reference steel MANET II [12]; (b) absorbed Charpy impact energy vs. testing-temperature diagram for subsize specimens of the low activation steel OPTIMAX B; (c) absorbed Charpy impact energy vs. testing-temperature diagram for subsize specimens of the renormalized, low activation steel OPTIMAX A renorm.

and they give rise to the identities $F \exp 1M'[e'(z)] = FiM1'[e'(z)]$ and $F \exp 2M'[e'(z)] = FiM2'[e'(z)]$. The latter two identities always reveal types of fracture, which are characterized by the absence of unstable crack propagation; in the case of ferritic-martensitic steels, this property is equivalent to ideal plasticity. Thus, the maximum impact line-forces, which are achieved prior to rupture, are independent of the initial defect-size distribution for ideal materials, i.e. the fracture processes leading to failure are fully controlled by

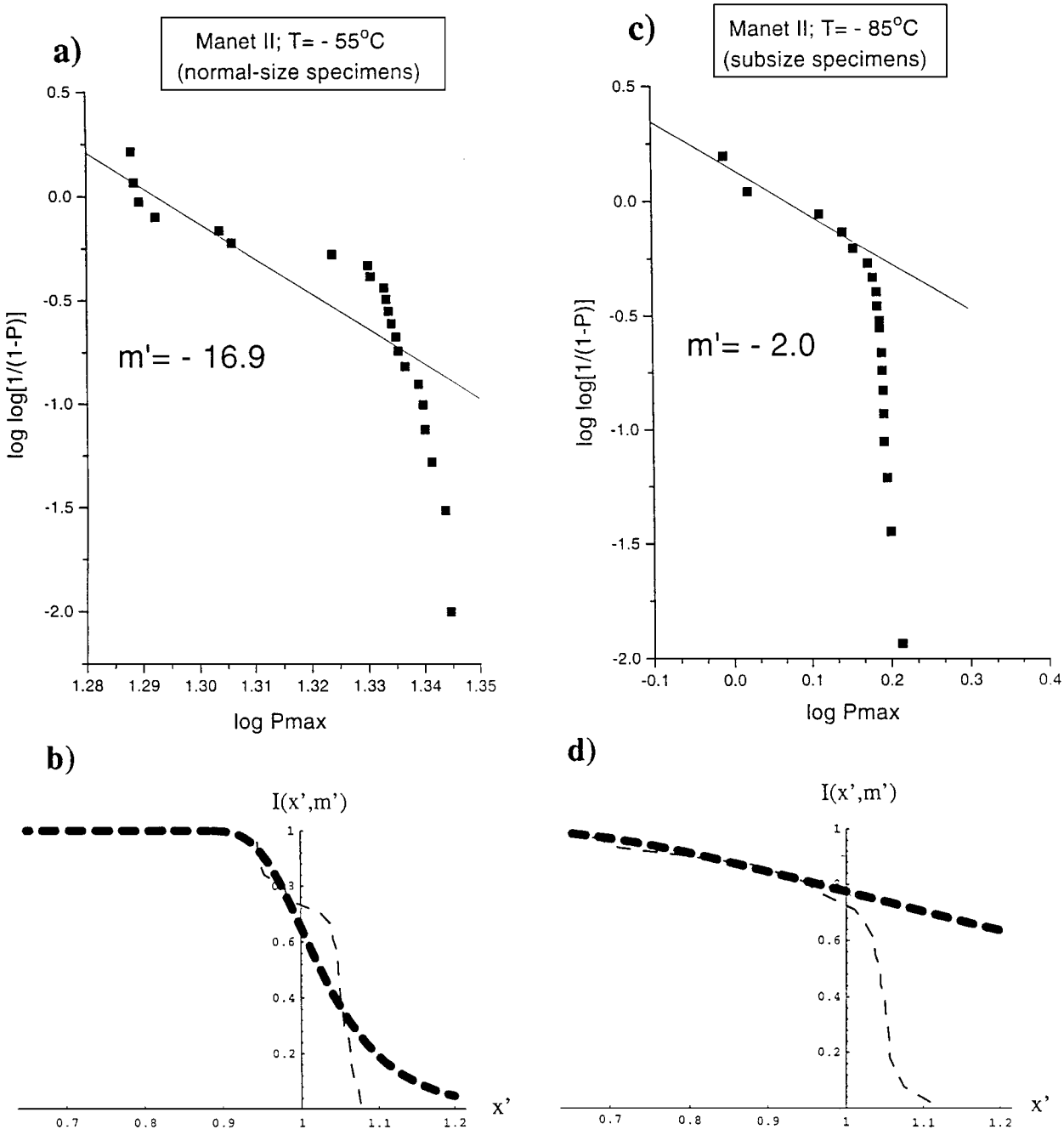

Figure 2 (a) Dynamic Weibull plot of Charpy impact tests of MANET II being performed at $-55\,^{\circ}$C with normal-size specimens; (b) Thick, dashed line: Theoretical dynamic Weibull master curve $I(x', m' = -16.9)$ of normal-size specimens of MANET II. Thin, dashed line: Experimental dynamic Weibull master curve $I\exp(x', m' = -16.9)$ of normal-size specimens of MANET II; (c) Dynamic Weibull plot of Charpy impact tests of MANET II being performed at $-85\,^{\circ}$C with subsize specimens; (d) Thick, dashed line: Theoretical dynamic Weibull master curve $I(x', m' = -2.0)$ of subsize specimens of MANET II. Thin, dashed line: Experimental dynamic Weibull master curve $I\exp(x', m' = -2.0)$ of subsize specimens of MANET II.

the toughening mechanisms being responsible for the occurence of stable crack growth. Possible toughening mechanisms might be crack-deflection, crack-bridging, crack-branching, network-formation and microcracking, mechanically induced phase-transformations, martensitic transformations, twinning, plastic matrix-yielding, (micro)crack-induced localized plasticity, ductile tearing, interface- or grainboundary-sliding etc. as well as combinations of mechanisms of this selection. The toughening mechanisms might be relevant in the reduction of the nucleation-rate of (micro)cracks from initial defects, in crack-tip shielding and the consequent arrest of large cracks and/or in the promotion of the stable growth of (micro)cracks. The initial defects, being intrinsic or being produced by irradiation, prestraining, preloading etc., always represent the potential starting points for the nucleation of microcracks. On the other side, finite values of $F\exp 1M'[e'(z)]$ and $F\exp 2M'[e'(z)]$ refer to fracture events with a limited percentage of stable crack extension, whereas pure brittle cleavage fracture is characterized by $F\exp 1M'[e'(z)]$ and $F\exp 2M'[e'(z)]$ being equal to zero.

In part 3 [4], it has already been proved, that the two-component model of Cook and Clarke (CCM) can be used to interprete the Weibull parameters, which were evaluated as well from quasi-static tensile or bend tests as from dynamic Charpy impact tests. The

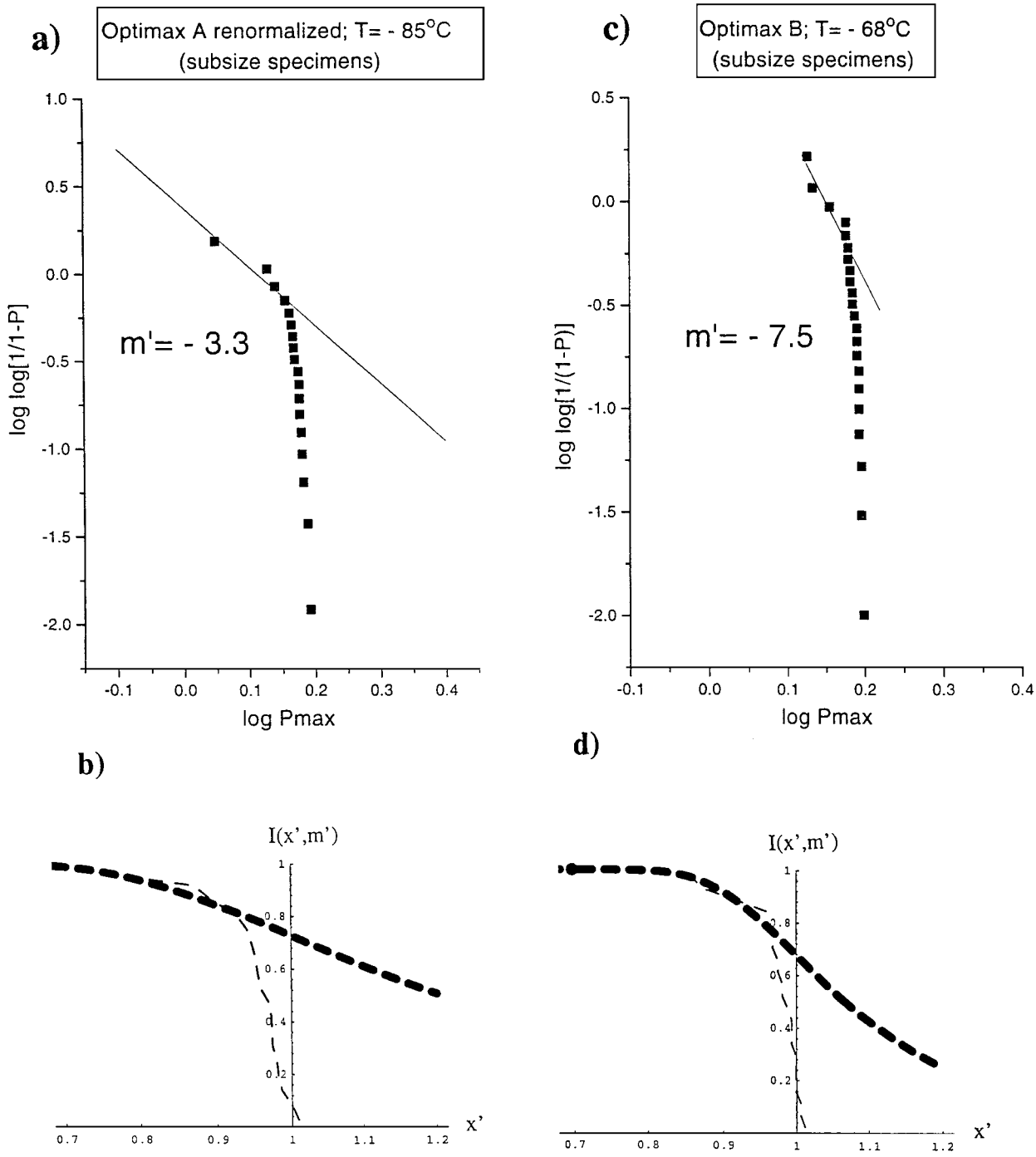

Figure 3 (a) Dynamic Weibull plot of Charpy impact tests of OPTIMAX A renorm. being performed at $-85\,^{\circ}$C with subsize specimens; (b) Thick, dashed line: Theoretical dynamic Weibull master curve $I(x', m' = -3.3)$ of subsize specimens of OPTIMAX A renorm. Thin, dashed line: Experimental dynamic Weibull master curve $I\exp(x', m' = -3.3)$ of subsize specimens of OPTIMAX A renorm.; (c) Dynamic Weibull plot of Charpy impact tests of OPTIMAX B being performed at $-68\,^{\circ}$C with subsize specimens; (d) Thick, dashed line: Theoretical dynamic Weibull master curve $I(x', m' = -7.5)$ of subsize specimens of OPTIMAX B. Thin, dashed line: Experimental dynamic Weibull master curve $I\exp(x', m' = -7.5)$ of subsize specimens of OPTIMAX B.

CCM is always significant, if residual stress fields arise because of localized deformations or localized loadings [10]. If the CCM is used to interprete the areas $F\exp 1M'[e'(z)]$ and $F\exp 2M'[e'(z)]$, it can be seen that, within the framework of this approach, values, shapes and positions of these areas are only dependent on the toughening exponent τ, describing the rising R-curve behaviour [4, 10], and on the type, localization and number of residual stress-fields existing in the process zone. The toughening exponent τ is uniformally valid and is, therefore, a characteristic value of the material, although it is specimen-size-dependent. In the case of Charpy impact testing, the localized component of the stress intensity factor in the CCM [4] is attributed to the maximum impact reaction line-force $P'_{\max}$ at the notch-tip of the specimens producing the residual stress fields inside the process zone. These residual stress fields are expected to determine mainly the $e'_{\mathrm{cr}}(z)$-value as well as the shape, value and position (relative to the $e'(z)$-axis) of $F\exp 1M'[e'(z)]$, whereas τ is assumed to influence predominantly the value of $F\exp 2M'[e'(z)]$. Under Charpy impact

TABLE I Chemical analysis of the alloys in wt %

	MANET II [12]	OPTIMAX A renom.	OPTIMAX B
Al	0.006	<0.02	<0.02
As	0.010	<0.005	<0.005
B	0.0089	0.0061	0.0061
Bi	—	0.005	0.005
C	0.11	0.094	0.09
Ce	—	0.036	0.033
Cr	10.3	9.24	9.42
Fe	Basis	Basis	Basis
Mn	1.22	0.56	0.037
Mo	0.57	0.093	0.048
N	0.039	0.0007	0.0029
Nb	0.14	<0.005	<0.005
Ni	0.62	<0.01	<0.01
P	0.005	0.007	0.008
Si	0.27	<0.02	<0.02
Ta	—	0.08	0.08
V	0.20	0.24	0.23
W	—	0.96	0.97

conditions, being typical for the DBTT-range of ferritic-martensitic steels, the localized stress-fields inside the process zone and, therefore, $e'_{cr}(z)$ and $F \exp 1M'[e'(z)]$, are believed to determine, in a first approach, the dynamic toughening behaviour of brittle materials with respect to stable microcracking in the medium $e'(z)$-range (see Fig. 2); for the stable growth of microcracks in the process zone is controlled by microstructural features. The toughening exponent τ, on the other hand, is thought to determine predominantly the toughening behaviour (i.e. the increased fracture resistance with increasing crack-size) of relatively large- and medium-size cracks in the higher $e'(z)$-range; for the stable propagation of the large, critical cracks being the origin for the final brittle fracture events after having undergone a considerable amount of stable crack-growth, might be mainly controlled by the continuum properties of the material. In agreement with the CCM a high $F \exp 2M'[e'(z)]$-value can be considered as a reliable shielding of the crack-tips of large- and medium-size cracks. Moreover, a high $F \exp 1M'[e'(z)]$-value being combined with $e'_{cr}(z) \approx 1$ indicates a huge amount of simultaneous, stable growth of microcracks as well as a narrow initial defect-size distribution [7, 11]; for if the initial defect-size distribution had not been narrow, $e'_{cr}(z)$ would have been increased clearly above one because of predominant rupture at quite high $e'(z)$-values being caused by the defects undergoing stable growth during loading and belonging to the large-size tail of the initial defect-size distribution. However, a $e'_{cr}(z)$-value, which is clearly larger than one, together with a high $F \exp 1M'[e'(z)]$-value is assumed to be the consequence of a wide initial defect-size distribution and an intense, simultaneous, stable growth of (micro)cracks of a wide size-range. This situation is typically expected, if debonding occurs along inhomogenities, such as grain-boundaries, interfaces, triple-point etc, being characterized by local, detrimental defect-size distributions or even increased concentrations of defects. Besides, the quasi-static deviation parameters $F \exp 1M[e(z)]$, $FiM1[e(z)]$, $F \exp 2M[e(z)]$, $FiM2[e(z)]$ and χ_M have been interpreted in a similar way as the dynamic deviation parameters [5]. However, a negative shift of the dynamic $e'_{cr}(z)$-value corresponds to a positive shift of the quasi-static $e_{cr}(z)$-value and vice versa. This asymmetry is the consequence of the indirect correspondence between the dynamic variable P_{max} and the quasi-static variable σ being expressed by Equation 20 of part 3 of this series of papers [4]. Thus, $I(x'_i, m') = 0.5$ means that the cumulative probability of failure due to scaled maximum impact line-forces $x' \geq x'_i$ is equal to 50%, whereas $I(x_i, m) = 0.5$ means that the cumulative probability of failure due to scaled, applied uniaxial tensile stresses $x \leq x_i$ is equal to 50%.

The positions of $F \exp 1M'[e'(z)]$ and $F \exp 2M'[e'(z)]$ relative to the $e'(z)$-axis, their shapes and values as well as the $e'_{cr}(z)$-value, could provide additional information about the toughening mechanisms operating in macroscopically homogeneous materials undergoing stable crack growth prior to failure, if experimental data of materials of known toughening mechanisms are available as calibration curves. On the other side, it is obvious that $F \exp 1M'[e'(z)]$ and $F \exp 2M'[e'(z)]$ of ferritic-martensitic steels are highly testing-temperature-dependent in the DBTT-rang, i.e. both deviation parameters are clearly decreasing with decreasing testing-temperature indicating a general increase of brittleness.

In the case of metals, the τ-value is an indicator for the capacity of the investigated materials to undergo stable crack-growth prior to failure, if the mobility of glissile dislocations is heavily reduced, for instance by high densities of small irradiation defects or by low testing-temperatures. The toughening exponent τ is evaluated from the lower P_{max}-range, corresponding to brittle cleavage fracture events starting from a minimum process zone. Besides, the testing-temperature must be chosen high enough in order to facilitate the formation of at least a minimum process zone; for only a process zone enables the occurrence of stable crack growth and, therefore, the evaluation of m' and τ by using the dynamic quasi-equilibrium approach (DQEA) presented in part 3 [4]. τ is approximately temperature-independent, if the DQEA is valid; for τ denotes the rate of toughness increase with increasing crack length c in the low temperature regime of the investigated ferritic-martensitic steels. This low temperature regime is characterized by the absence of significant testing-temperature-dependent toughening mechanisms, being the result of an efficient immobilization of the glissile dislocations in the glide planes at temperatures clearly lower than the DBTT. Thus, the toughening exponent τ is a low-temperature value with respect to the Charpy energy vs. testing-temperature diagrams depicted in Fig. 1. τ is related to fracture processes being characterized by toughening mechanisms, which work in the absence of any plastic matrix-yielding, i.e. in the absence of any mobility of glissile dislocations. Therefore, τ is a significant magnitude in order to estimate DBTT-shifts due to irradiation embrittlement; for the high densities of small defects in metals having been irradiated by fusion neutron spectra or equivalent proton spectra, mainly result in a

reduction of the mobility of glissile dislocations, i.e. in a reduced ductility in tensile tests [12, 13].

The dynamic quotients $d\chi_M$ are also assumed to be temperature-independent at least in the DBTT-range, if the DQEA is valid. The DBTT-range is defined by the requirement that the inherent scatter-range of the measured maximum impact line-forces P_{max} (and fracture energies) of series of Charpy impact tests, having been performed at any fixed testing-temperature in the DBTT-range, must be clearly larger than the changes of the corresponding mean-values, which occur if the testing-temperatures are varied in the DBTT-range. This criterium is equivalent to the fact, that there exists a considerable scatter of P_{max} being mainly a function of the initial defect-size distribution. It guarantees, that brittle failure occurs in a time-range, where stable crack propagation in the process zone is due to a nearly constant normal stress σ, which is activating the same toughening mechanisms for crack-tip shielding (of large- and medium-size cracks) and stable microcracking. Both fracture processes, being related to $F \exp 2M'[e'(z)]$ or $F \exp 1M'[e'(z)]$, respectively, lead to stress-release in the process zone and, therefore, to a delay of brittle failure. On the other side, the local stress-fields around initial defects and (micro)cracks inside the process zone differ considerably, since they are the result of a geometrical sensitive interaction with the local reaction line-force P'. Thus, P' is responsible for the formation of the process zone in the early load stages of the Charpy impact tests, and it also affects the final, dynamic cumulative critical crack-size distribution, which is strongly related to the local residual stress-fields around the initial defects in the process zone. The assumption of a testing-temperature-independent $d\chi_M$-value implicitly presumes the activation of the same toughening mechanisms for crack-tip shielding of large-size cracks and stable microcracking, resulting in the required weak and nearly identical temperature-dependence of the two processes. Therefore, it is also probable that $e'_{cr}(z)$ is only slightly temperature-dependent. Nevertheless, all the local stress-fields, which have been built up during the formation of the process zone by P', are expected to be highly sensitive to the testing-temperature even in the DBTT-range; for they are formed near the notch-tip under the influence of intense longitudinal waves by dynamic, partially adiabatic and plastic processes [4] being mainly based on a remaining mobility of glissile dislocations due to localized, adiabatic heating. Because of the local, temporal, partially adiabatic regime, a minimum dislocation mobility is still existing near the notch-tip in the whole DBTT-range, at least during the earliest inertia-affected load stage of Charpy impact tests.

In order to determine $d\chi_M$, the testing-temperature should be chosen high enough to guarantee detectable deviation areas $F \exp 2M'[e'(z)]$ and $F \exp 1M'[e'(z)]$. On the other side, the testing-temperature should be also low enough to facilitate the evaluation of the full shapes of $F \exp 2M'[e'(z)]$ and $F \exp 1M'[e'(z)]$ without exceedingly high statistical requirements [5]. In addition, the testing-temperature should also be quite low in order to obtain a sufficiently large lower P_{max}-range being characterized by purely brittle fracture, thus enabling the evaluation of the dynamic Weibull moduls m'. However, direct comparisons of the dynamic quotients $d\chi_M$ of different materials with heavily varying m'-values remain to be difficult, as long as calibration curves $d\chi_M(m')$ are not available and as long as it is not clear up to which degree $d\chi_M$ is shape- and $e'_{cr}(z)$-dependent.

4. Results and discussion

4.1. Charpy impact testing in the DBTT-range

The results of the Charpy impact tests, being performed with normal-size and subsize specimens are gathered in Table II. All the experimental results have been evaluated on the basis of the special dynamic Weibull master curves $I(x', m')$ and $I \exp(x', m')$ for reasons already mentioned in part 3 of this series of papers [4]. Simple, optical inspection of the fracture surfaces of normal-size specimens, which had been tested by performing Charpy impact tests in the upper DBTT-range of the corresponding materials, confirmed that fracture has taken place predominantly under plane strain conditions; for mainly square fracture was observed, whereas the shear lips were negligible [14]. On the other side, it had been found that the fracture surfaces of subsize specimens, which had been tested under similar conditions as the normal-size specimens, always showed considerable shear-lips. This fact indicates, that a significant part of the fracture process of subsize specimens occurred under plane stress or transitional conditions [14].

TABLE II Dynamic Weibull parameters derived from Charpy impact tests

	Normal-size specimens of MANET II	Subsize specimens of MANET II	Subsize specimens of OPTIMAX A renorm.	Subsize specimens of OPTIMAX B
Testing-temperature (°C)	−55	−85	−85	−72
DBTT (°C)	—	−45 [12]	−82	−55
$\frac{F \exp 1M'[e'(z_{in})]}{Fi M1'[e'(z_{in})]}$	0.215	≈0	≈0	≈0
$\frac{F \exp 2M'[e'(z_{in})]}{Fi M2'[e'(z_{in})]}$	0.833	0.913	0.902	0.895
$d\chi_I$	3.874	∞	∞	∞
x'_{cr}	1.05	0.94	0.90	0.97
m'	−16.9	−2.0	−3.3	−7.5
τ	0.07	0.42	0.37	0.25

In order to calculate the toughening exponent τ with the help of m', the quasi-static Weibull modulus m has to be known. An m-value of 22 has been used, since this value has been found to be typical for nuclear pressure vessel steels [15]. Furthermore, the m-values of the three investigated ferritic-martensitic steels are expected to differ only very weakly, since their microstructures, especially the carbide densities and carbide size-distributions, are very similar, as a result of specially designed heat treatments [8, 9]. Consequently, the same might also be expected for the corresponding inhomogeneities in flaws to trigger fracture and, therefore, the width of the (normalized) initial defect-size distributions being characterized by the quasi-static Weibull modulus m [16–18]; for Cr-rich carbides are mostly considered as being the initial defects acting as sources of microcracks in Cr-rich ferritic-martensitic steels like MANET II and the OPTIMAX steels [19].

According to Table II, the MANET II steel shows a high testing-temperature-independent $d\chi_I$-value, if normal-size specimens are tested. Moreover, x'_{cr} is clearly larger than one. Both results might be interpreted as the result of debonding, occuring along the crystallographically sharp interfaces of the martensite laths mainly under bulk-specific plain strain conditions [11, 14]. Nevertheless, the nucleation sites of (micro)cracks might still be related to carbides as reported by Curry and Knott [20]. The large value of $F \exp 1M'[e'(z_{in})]$ marks a reduced influence of the initial defect-size distribution because of the strong capacity to undergo stable microcracking prior to failure. The high capacity of microcracking is even supplemented by an efficient shielding of crack-tips of large- and medium-size cracks, being quantified by the quite high $F \exp 2M'[e'(z_{in})]$-value. Thus, it is assumed that irradiation of ferritic-martensitic steels with neutrons, protons etc. producing microstructures with high defect-densities [13] results in a smaller DBTT-shift due to irradiation embrittlement, if the capacity of stable (micro)cracking in the DBTT-range is considerable; for the irradiation-induced reduction of the mobility of dislocations by high defect-densities being detrimental for the capacity of shielding of crack-tips by dislocation mechanisms [21] and probably being the main reason for high DBTT-shift due to irradiation, could in this case, at least partially, be compensated by shielding mechanisms, which are based on stable (micro)cracking or by (micro)crack-induced, local plasticity. These considerations are experimentally supported by the fact that the irradiation-induced DBTT-shifts of MANET II are quite small in comparison, for example, to iron [12]. Pure iron is expected to have a clearly minor capacity to undergo stable (micro)cracking than the ferritic-martensitic steel MANET II.

4.2. Discussion of the dynamic deviation parameters of subsize specimens

The gradient of the normal stress σ, which is built up during Charpy impact tests according to the DQEA, is larger is subsize specimens than in normal-size specimens, whereas the volume of the process zone is smaller in DIN 50115 KLST subsize specimens than in normal-size ISO-V-specimens. Moreover, τ is about six times larger in the case of subsize specimens of MANET II (see Table II). The low σ-gradient and the relatively large volume of the process zone of normal-size specimens favour simultaneous stable growth of defects and microcracks of various sizes, resulting in the observed high $F \exp 1M'[e'(z_{in})]$-value, whereas the opposite is true for subsize specimens; for large σ-gradients combined with small process zones only provide statistically insufficient numbers of initial defects being exposed to nearly equivalent normal stress conditions in order to enable the application of the dynamic Weibull theory. Thus, the $F \exp 1M'[e'(z_{in})]$-value of subsize specimens merely represents a lower limit. However, the $F \exp 1M'[e'(z_{in})]$-value might even be underestimated in the case of normal-size specimens, since the number of the involved defects could still be statistically insufficient in order to represent the full shift of the dynamic, cumulative initial defect-size distribution function. Besides, this shift can arise, if stable (micro)cracking occurs prior to brittle failure. The shifted dynamic, cumulative initial defect-size distribution represents the dynamic, cumulative critical (micro)crack-size distribution [7, 10].

The $F \exp 1M'[e'(z_{in})]$-value of subsize specimens, is nearly zero according to Table II. Therefore, it can be concluded, that the initial defect-size distributions of subsize specimens are hardly altered by stable microcracking during Charpy impact testing. A further consequence of the geometrical restrictions of subsize specimens is the impossibility of evaluating the testing-temperature-independent double-quotient $d\chi_I$ ($d\chi_I$ becomes always infinite in the considered cases, because the $F \exp 1M'[e'(z_{in})]$-value of the tested subsize specimens is equal to zero). The increased τ-values of subsize specimens (see Table II) can be explained by the increased influence of plane stress and transitional conditions being most important in the near-surface regions of the process zone [14]. On the other side, deviations from the bulk-specific plane strain conditions are thought to be negligible in the case of normal-size specimens.

The $F \exp 2M'[e'(z_{in})]$-values are related to the reliability of shielding of large- and medium-size cracks without explicitly revealing the role of plastic matrix-yielding. The $F \exp 2M'[e'(z_{in})]$-value is dependent on both the toughening exponent τ and the plastic matrix-yielding, which takes place at the crack-tips of large- and medium-size cracks. The latter, is also influencing the cross-over values x'_{cr}. Consequently, the geometrical restrictions of subsize specimens are expected to affect the x'_{cr}-value. Furthermore, x'_{cr} might also be slightly testing-temperature-dependent, especially under the plane stress and transitional conditions of subsize specimens. The measurements of the cross-over values x'_{cr}, being often shifted to values below one in the case of subsize specimens (see Table II), may be explained in this way.

The shielding of large- and medium-size cracks in the absence of matrix-plasticity, being characterized by τ, is usually highly increased in subsize specimens;

for the high τ-value is equivalent to a steep R-curve, which guarantees increased stable (micro)cracking and (micro)crack-induced shielding. Furthermore, it is also probable that the crack-tips of large- and medium-size cracks are additionally shielded in subsize specimens, because there always remains some localized, (micro)crack-induced plasticity in the near-surface regions, even in the lower DBTT-range. This localized plasticity, which is possibly decreasing the x'_{cr}-value of subsize specimens, might be so extraordinary efficient in shielding crack-tips of the large, critical cracks, since it is strongly interacting with other toughening mechanisms under plane stress or transitional conditions.

4.3. Dynamic Weibull master curves

In the case of quasi-static Weibull master curves, a small cross-over value $x_{cr} < 1$ means a low failure rate at low applied normal stresses, whereas $x'_{cr} < 1$ means a relatively decreased failure rate at high maximum impact line-forces P_{max}, if dynamic Weibull master curves are concerned. $x'_{cr} < 1$ always indicates a microstructure, which is favourable with regard to the shielding of crack-tips of large- and medium-size cracks, if normal-size specimens are tested. On the other side, the lack of stable microcracking in subsize specimens might be a reason for the geometrically induced reduction of the x'_{cr}-value being observed for MANET II (see Fig. 2). Furthermore, $x'_{cr} < 1$ might also be the result of plane stress and transitional conditions in the near-surface regions of the process zones of subsize specimens, giving rise to high toughening exponents τ, high $F \exp 2M'[e'(z_{in})]$-values, steep R-curves and, consequently, additional shielding of large- and medium-size cracks in the upper and lower P_{max}-range. The geometrical shielding effect in subsize specimens is increasing with decreasing distance from the surfaces of the specimens [14]. It is best modelled by additional residual stress fields, which have high compressive components in the near-surface regions and which overlap the corresponding bulk-material being characterized by plane strain conditions [10, 14]. Therefore, the evaluated toughening exponent τ of subsize specimens merely represents a material- and geometry-specific mean-value.

If a small $F \exp 1M'[e'(z_{in})]$-value and a cross-over value $x'_{cr} \approx 1$ is evaluated from tests with normal-size specimens, it mostly means that stable growth of defects and (micro)cracks only occurred at a low level during the Charpy impact tests. However, if $x'_{cr} \approx 1$ is combined with a considerable high $F \exp 1M'[e'(z_{in})]$-value in the case of normal-size specimens, it might indicate intense, stable microcracking as well as a narrow initial defect-size distribution. Besides, the initial defect-size distributions is also characterized by the quasi-static Weibull modulus m [16–18].

$x'_{cr} > 1$ being combined with an insignificant $F \exp 1M'[e'(z_{in})]$-value indicates lack of microcracking as well as a weak shielding of crack-tips of large- and medium-size cracks for both normal-size and subsize specimens. In addition, there might have also been only a week formation of residual stress fields in the process zone by dynamic, partially adiabatic and plastic deformations during the early inertia-affected load stage [4].

$x'_{cr} > 1$ in combination with a large $F \exp 1M'[e'(z_{in})]$-value indicates simultaneous stable growth of a wide size-range of defects and (micro)cracks prior to brittle failure. This interpretation is valid for normal-size as well as subsize specimens. The described characteristics is typical for debonding phenomena, such as intercrystalline cracking, (micro)cracking along boundaries of different phases, martensite laths or twins, (micro)cracking along interfaces or domains etc. Significant debonding is thought to take place only in normal-size specimens of MANET II, but not in the corresponding subsize specimens; for only in the case of normal-size specimens intense, stable microcracking, which could trigger debonding along martensite laths, has been observed to occur prior to rupture, if the Charpy impact tests are performed in the DBTT-range (see Fig. 2).

4.4. Geometrically induced DBTT-shifts

The DBTT is shifted to lower temperatures for geometrical reasons, if subsize specimens are tested instead of normal-size specimens. This geometrical shift is supposed to be the consequence of a strongly improved, temperature-sensitive, plastic shielding of the crack-tips of large- and medium-size cracks, if they become large enough to contact the near-surface regions of the process zones of subsize specimens after having undergone an amount of stable crack-growth. The crack-tip shielding by dislocations is highly temperature-sensitive in the DBTT-range [21], and it is more efficient in subsize than in normal-size specimens, especially in the lower DBTT-range; for the near-surface regions of the process zone, which are only relevant for subsize specimens and which give rise to plane stress and transitional conditions, in a significant volume of the process zone [14], probably undergo plastic matrix-yielding down to clearly lower temperature than bulk-material being characterized by plane strain conditions [14]. The fracture process of normal-size specimens, on the other side, essentially takes place under plane strain conditions. The described geometry-effect is quite strong, since the critical cracks, which trigger brittle failure, extend over the whole width of the process zone, at least close to the onset of final, brittle fracture. Consequently, it can be assumed that the geometrically induced DBTT-shifts of irradiated steels are less striking than the corresponding DBTT-shifts of unirradiated ones, because irradiated specimens are generally characterized by a strong reduction of the highly testing-temperature-dependent dislocation mobility, as a result of irradiation embrittlement. Therefore, stable (micro)cracking and (micro)crack-induced shielding mechanisms, which are less sensitive to testing-temperature and geometrical effects than matrix-plasticity, turn out to be much more important for irradiated steels than for unirradiated steels with respect to fracture toughness.

4.5. Charpy impact tests of subsize specimens

None of the tested materials showed significant microcracking prior to failure, if subsize specimens were tested, since $F \exp 1M'[e'(z_{in})] \approx 0$ was always true according to Figs 2 and 3. Therefore, the testing-temperature-independent double-quotients $d\chi_I$ always became infinite. These discoveries are in strong contrast to the results evaluated from normal-size specimens of MANET II, being characterized by a much larger process zone, a smaller σ-gradient and neary pure plane strain conditions. Moreover, the $F \exp 2M'[e'(z_{in})]$-values are strongly dependent on the exact testing-temperature and are, therefore, not convenient in order to compare alloys with different DBTTs, especially if finite testing-temperature-independent double-quotients $d\chi_I$ cannot be evaluated.

MANET II, the ferritic-martensitic steel containing clearly higher nitrogen- and manganese-contents but lower tungsten-contents than the OPTIMAX steels, is thought to be highly efficient in shielding of crack-tips of large- and medium-size cracks in the absence of matrix-plasticity; for its τ-value is nearly maximum, if subsize specimens are tested. The x'_{cr}-value is clearly below one, possibly indicating that the excellent shielding of large- and medium-size cracks might also be a consequence of (micro)crack-induced, localized plasticity in the near-surface regions of the subsize specimens. The $F \exp 2M'[e'(z_{in})]$-value is strongly dependent on the exact testing-temperature and is, therefore, not convenient in order to compare alloys with different DBTTs. OPTIMAX B, being mainly characterized by the lowest manganese-content of all the investigated steels, shows a clearly lower capacity of shielding than MANET II, because its τ-value is much smaller and its x'_{cr}-value larger than the corresponding values of MANET II. OPTIMAX A renorm., being characterized by the lowest nitrogen-content of all considered steels, shows clearly the narrowest DBTT-range (see Fig. 1) and the lowest x'_{cr}-value. The very narrow DBTT-range could be the result of high cleanliness, whereas the low x'_{cr}-value indicates that shielding is probably due to intense, localized, (micro)crack-induced plasticity in the near-surface regions of the process zone. The total shielding effect in the absence of any matrix-plasticity, being characterized by τ, is also considerable, although it is less efficient in OPTIMAX A renorm. than in MANET II.

DBTT-shifts due to irradiation embrittlement are probably reduced, if the material has a high capacity of stable (micro)cracking prior to failure as well as a good capacity of shielding of crack-tips of large- and medium-size cracks in the absence of matrix-plasticity. Both properties are certainly to be related to the corresponding capacity of shielding in the presence of full matrix-plasticity, being quantified by the Charpy energies of the high temperature-range (see Fig. 1). Thus, it is supposed that the low activation steels OPTIMAX A renorm. and, most of all, OPTIMAX B undergo a larger DBTT-shift due to irradiation embrittlement than MANET II. It has implicitly been assumed that the capacity of shielding of large- and medium-size cracks in the absence of matrix-plasticity being quantified by τ, is positively correlated to the capacity of stable microcracking, since both processes are expected to be based on the same toughening mechanisms. Nevertheless, the capacity of undergoing stable microcracking prior to failure has not been measured explicitly for the OPTIMAX steels, because only Charpy impact tests with subsize specimens have been performed.

5. Conclusions

A high capacity of stable (micro)cracking prior to failure may be an important mechanical property for structural steels in fusion technology, since it possibly decreases the DBTT-shifts of ferritic-martensitic steels, which result as a consequence of (neutron)irradiation embrittlement. On the other side, there might exist alloys undergoing quite an amount of stable (micro)cracking prior to failure, by activating such types of toughening mechanisms, which reduce their DBTT-shifts due to irradiation embrittlement, but affect their creep and fatigue properties in an essentially negative manner; for the reduction of the DBTT-shifts, being measured by performing Charpy impact tests, is a highly dynamic, short-term effect, whereas the creep and fatigue properties are the consequence of long-term processes. Thus, (micro)crack-nucleation, crack-tip shielding, stable (micro)cracking, crack branching etc. occurs in creep and fatigue tests under completely different physical conditions than in Charpy impact tests.

It is very likely, that DBTT-shifts due to irradiation embrittlement are minimum for steels with high capacities of both stable (micro)cracking and crack-tip shielding in the lower DBTT-range; for the lower DBTT-range is characterized by the absence of matrix-plasticity.

The amount of crack-tip shielding of large- and medium-size cracks in the absence of plastic matrix-yielding, being quantified by the toughening exponent τ, seems to be crucial for subsize specimens in order to estimate irradiation-induced DBTT-shifts, whereas for normal-size specimens both the amount of stable microcracking prior to failure and the amount of crack-tip shielding are supposed to be essential for this purpose.

References

1. R. L. KLUEH, K. EHRLICH and F. ABE, *J. Nucl. Mater.* **191** (1992) 116.
2. N. S. CANNON and D. S. GELLES, *ibid.* **186** (1991) 68.
3. K. KROMPHOLZ, P. TIPPING and G. ULLRICH, *Z. Werkstofftech.* **15** (1984) 199.
4. M. LAMBRIGGER, part 3 of this series of papers, submitted to *J. Mater. Sci.*
5. *Idem.*, part 2 of this series of papers, *ibid.*, to be published.
6. *Idem.*, part 1 of this series of papers, *ibid.*, to be published.
7. R. F. COOK and D. R. CLARKE, *Acta Metall.* **36** (1988) 555.
8. P. MARMY, *Plasma Devices and Operations* **4** (1996) 211.
9. M. VICTORIA, D. GAVILLET, P. SPATIG, F. REZAIARIA and S. ROSSMANN, *J. Nucl. Mater.* **233–237** (1996) 326.
10. M. LAMBRIGGER, *J. Mater. Sci. Lett.* **16** (1997) 298.
11. *Idem.*, *Phil. Mag.* **A77** (1998) 363.
12. I. BELIANOV and P. MARMY, to be published in Proceedings of ICFRM-8, October 26–31, 1997 (Sendai, Japan).
13. Y. DAI, Thèse No. 1388, Ecole Polytechnique Fédéral de Lausanne, 1995.

14. D. BROOK, in "Elementary Engineering Fracture Mechanics" (Martinus Nijhoff Publishers, Dordrecht, 1987) pp. 179–227.
15. F. M. BEREMIN, *Metall. Trans.* **A14** (1983) 2277.
16. W. WEIBULL, Ingeniörvetenskapakademien, Handlingar No. 151, Stockholm, 1939.
17. K. WALLIN, *Eng. Fract. Mech.* **19** (1984) 1085.
18. K. KENDALL, N. MCN. ALFORD, S. R. TAN and J. D. BIRCHALL, *J. Mater. Res.* **1** (1986) 120.
19. G. E. LUCAS, H. YIH and G. R. ODETTE, *J. Nucl. Mater.* **155–157** (1988) 673.
20. D. A. CURRY and J. F. KNOTT, *Met. Sci.* **12** (1978) 511.
21. S. G. ROBERTS, M. ELLIS and P. B. HIRSCH, *Mater. Sci. Eng.* **A164** (1993) 135.

Received 22 September 1998
and accepted 2 March 1999